

Deformation law and stability state of cofferdam during pumping process in PC combined method pile cofferdam

Funing Li, Jie Huang*

Department of Construction and Real Estate, School of Civil Engineering, Southeast University, Nanjing 211189, China, email: huangj0316@163.com (J. Huang)

Received 24 August 2023; Accepted 30 October 2023

ABSTRACT

Cofferdam is a key component of the containment system during the construction period. In order to ensure the quality and safety of underground open cut structure projects in China, and to strongly promote the development and progress of similar underground engineering cofferdam technology such as open cut lake tunnels, this paper takes the Jinji Lake tunnel cofferdam project as the basis, and conducts a study on the deformation law and stability state of PC combined method pile cofferdam support structure during the whole process of weir pumping construction combined with field monitoring analysis. The results show that: (1) with the continuous pumping and slope excavation, the overall structural deformation of the cofferdam tends to move more and more towards the inner side of the cofferdam; (2) during the construction process, the horizontal displacement values of the pile tops on the waterward and backward sides of the cofferdam do not differ much; and the maximum horizontal displacement value of the pile body on the waterward side does not differ much from the horizontal displacement value of the pile top, but on the backward side differs significantly. (3) During the pumping process in the weir, the maximum horizontal displacement of the piles on both sides of the weir basically appears near the bottom of the lake. The study reveals the asymmetric deformation law of the piles on both sides of the weir, which provides reference for similar projects of PC combined method pile cofferdam.

Keywords: PC combined method pile cofferdam; Deformation law; Stability; Finite element simulation; Field monitoring

1. Introduction

As a new type of support structure, PC construction method pile is a combination of Larsen steel sheet pile and steel pipe pile to form composite piles with different sections. The lock catch uses shaped Larsen steel sheet as the lock catch, which has simple manufacturing process, high degree of industrialization and automation, good water stopping effect, relatively easy control of driving perpendicularity, high construction efficiency, and guaranteed quality. Compared to ordinary lock catch steel cofferdam, it has greater rigidity and less deformation. The amount of steel used is also relatively small. PC construction method

piles have a wide range of uses. Compared to earth-rock cofferdam and traditional steel sheet piles, PC construction method piles have many advantages, such as high sectional strength, good durability, good weather resistance, good water sealing effect, as well as no pollution during the entire process of use, convenient construction, fast acceptance, and recyclability. They are valued and favored by the cofferdam field. Currently, there are two main calculation and design methods in the research of steel cofferdam and steel sheet pile at home and abroad: simplified calculation method and finite element calculation method.

Currently, there are no clear regulations on the design of double row steel cofferdams, which are still in a semi theoretical and semi empirical state. Many experts and

* Corresponding author.

scholars have also conducted targeted research. Uribe-Henao and Arboleda-Monsalve [1] have studied the impact of installation of steel sheet pile cofferdam ring beams on the performance of urban cofferdams. Using three-dimensional numerical analysis, it is found that only after some deformation, the natural relaxation of interlocking and steel sheet pile ring beam connections will narrow their gaps, The support system can be fully engaged; based on the research and experience of the Mekong River Delta project, Quang et al. [2] calculated that the combination of cement columns and ordinary steel sheet piles for deep and wide foundation pit cofferdams is a reasonable solution; Verstov et al. [3] discussed the developed offshore waterproof steel sheet pile cofferdam technology for building artificial islands. The proposed technology can improve efficiency and shorten work completion time; Li et al. [4] introduced the design of the key parts of the USSP cofferdam under the action of tides, established a three-dimensional finite element model corresponding to all construction steps, conducted backtesting and analysis of the measured deflection of the USSP, and studied the effects of tidal level, soil parameters, support stiffness, and construction sequence on the lateral deflection of the USSP. The results showed that the maximum deflection during construction occurred near the riverbed, extracting water before the concrete substrate can greatly improve construction efficiency; Wang et al. [5] established a support vector machine (SVM) medium and short term water level prediction model, using SVM tools to establish a prediction model that comprehensively considers complex hydrological scenarios and weather changes, making the medium and short term water level prediction more accurate, thereby achieving dynamic adjustment and better adapting to the actual needs of steel sheet pile cofferdam construction; Gui and Han [6] investigated the reasons for the failure of the double wall cofferdam during construction, introduced the failure background, failure situation, and the results of finite element analysis after failure, and finally pointed out the actual reasons for the failure; Hou et al. [7] analyzed the measured data, studied the deformation performance of large span double row steel sheet piles, and studied the impact of soil reinforcement technology on deformation control of double row steel sheet piles using a two-dimensional finite element method. Huang et al. [8] conducted control analysis on the stability calculation of double row steel sheet piles in soft soil foundation based on soil mechanics theory from aspects of uplift stability, overall sliding stability, anti overturning stability, and overall sliding stability of steel sheet piles. Through theoretical derivation and calculation, a formula for calculating the minimum penetration depth L_d of steel sheet piles is given; Xiong et al. [9] established a three-dimensional finite element model on steel sheet piles, purlins, inner bearings, and soil, and drew conclusions through calculating model values and monitoring values; Wang et al. [10] took the U-shaped steel sheet pile supporting foundation pit in the middle and lower reaches of the Yangtze River as an example, established a three-dimensional finite element model of the supporting structure, and conducted an RMA parameter analysis. Aiming at the uncertainty of the U-shaped steel sheet pile RMA in general situations, they

proposed an optimization strategy for the design of the U-shaped steel sheet pile supporting structure; Liu et al. [11] analyzed the working mechanism, design points, and construction points of the large diameter deep inserted steel tube structure through their research on the scheme of the large diameter deep inserted steel tube. Wu et al. [12] proposed a novel excavation and construction method for a lake crossing tunnel. They designed DSSPs cofferdams, dividing the excavation of the upper layer into several closed areas, and using a combination of finite element analysis and on-site monitoring data, providing a new idea for construction. Arboleda-Monsalve et al. [13] studied the impact of excavation under two different cofferdams, segmental steel ring beam support and cast-in-situ reinforced concrete ring beam support, on the ground. Haack [14] used advanced structural models to study the ground change rules caused by excavation of concrete supports in urban cofferdams. Spaans and Milutinovic [15] introduced the analysis and design methods of precast concrete cofferdams. The precast concrete cofferdam was subjected to finite element analysis and adequate inspection at all stages of construction. Pal et al. [16] focused on studying the settlement behavior of the cofferdam top through monitoring data, introducing a corresponding function to predict future settlement. Su et al. [17] combined with reclamation projects, studied the variation of shear strength and compressive modulus of soft soil under different degrees of consolidation through theoretical analysis, and used finite element methods to study the variation of vertical and horizontal ultimate bearing capacity of a single pile with the degree of soil consolidation. Fall et al. [18] evaluated the changes in the bending moment of the bottom wall, the lateral and vertical displacements of the top wall, and the reaction force of the anchor rod applied to the steel sheet pile through numerical studies. Azzam and Elwakil [19] studied the potential benefits of using pile retaining walls to resist axial loads. The results show that the ultimate axial bearing capacity of the test pile wall increases significantly with the increase of penetration depth and soil relative density. Through case studies and finite element results, Zheng et al. [20] have shown that inclined piles (IP) are more effective than vertical piles (VP), while composite inclined retaining structures (CIRS) are more effective than IP in reducing deflection and bending moments.

Many scholars have fully studied the calculation theory of stress and deformation of double row steel cofferdams [21–23] mainly from traditional calculation methods and finite element calculation methods, and have achieved many research results, which lays the foundation for further research in this article. However, due to the relatively novel support structure of the PC composite construction method pile cofferdam, there are some differences between the common double row steel sheet pile and steel pipe pile cofferdams [24–26]. Therefore, this paper uses finite element analysis software to analyze the deformation, strength, and stability of the steel pipe pile cofferdam structure to ensure the construction safety of the steel pipe pile cofferdam structure [27–29]. The deformation law and stability of the PC composite pile cofferdam support structure during pumping and excavation in the cofferdam were studied.

2. Project introduction

2.1. Project overview

The project is located in Wuzhong District, Suzhou City, crossing Jinji Lake in an east-west direction, the tunnel starts from Xinghai Street (including Xinghai Street intersection) in the west to Nanshi Street (including Nanshi Street intersection) in the east, with a total length of about 5.35 km, of which about 3 km is in the lake (including the rail transit co-construction section) and about 2.35 km is on land. 6 lanes in both directions on the main expressway, the calculated travel speed of the main line is 50 km/h, and the calculated travel speed of the ramp is the cofferdam and other temporary construction buildings are class 4 hydraulic buildings. The total length of cofferdam is about 6.8 km, and the elevation of the lake bottom is more than -1.00~ -6.00 m. The cofferdam is used as temporary water retaining structure for construction, and a thousand of them are constructed by open excavation method, and the plan of the tunnel project is shown in Fig. 1.

Steel pipe piles and SP-IV Larsen sheet piles are mainly used to form the weir. Φ720 steel pipes are used on the water side of the steel pipe pile weir, and the adjacent steel pipes are connected by “PC” type locking. SP-IV Larsen sheet pile cofferdam is mainly a temporary cofferdam with two layers of Larsen sheet piles spaced 8.0 m apart and filled with earth to form a cofferdam.

2.2. Geological conditions

The geomorphology of this area belongs to the Taihu Lake basin piled up the plain area of flat water network (II2a), the site topography is flat, the terrain slightly to the east, ground elevation 3–4 m, dense river network, the surface is mainly alluvial – lake phase, lake – marsh phase piled up soil layers in the upper horizontal distribution of the site is more stable, the stability of the lower soil layer is poor, the thickness of the fourth system cover layer in the site can be more than 180 and 75.30 m along the tunnel to shallow The soil layer is a loose sediment deposited from the Holocene to the early Pleistocene of the fourth system, mainly clayey soil, interspersed with powdery (sandy) soil. According to the physical and mechanical properties, deposition environment and genesis type of each soil layer, it can be divided into 11 engineering geological layers and 24 engineering top sub-layers, Table 1.

2.3. Hydrological conditions

- Surface water survey area surface water system development, the proposed tunnel route through the Jinji Lake, Lake Taihu water through the river source of continuous replenishment of Jinji Lake water, surface water another source of atmospheric precipitation, water level elevation changes mainly by the level of Lake Taihu, surrounding rivers and lakes and seasonal precipitation



Fig. 1. Plan of Jinji Lake tunnel project.

Table 1
Distribution of cofferdam soil layers

Serial No	Soil layer name	Layer thickness (m)	Severe (KN/m ³)	Elastic modulus	Poisson's ratio	Cohesion	Friction angle
1	Silt①	0.2	16.0	15,880	0.49	2.8	3.0
2	Silty clay② ₂	0.3	19.3	22,960	0.49	22.4	12.7
3	Silt③ ₃	2.8	19.2	24,720	0.48	8.0	28.7
4	Silt mixed with powder④	4.4	19.6	23,290	0.45	6.2	30.5
5	Silty clay⑤	9.1	19.1	30,560	0.39	21.5	12.4
6	Clay⑥ ₁	2.9	20.4	25,920	0.38	49.2	12.1
7	Silty clay⑥ ₂	4.5	19.9	27,280	0.42	29.2	13.6
8	Silt mixed with silty sand⑦	4.0	19.5	38,720	0.36	7.9	29.2
9	Filling	/	16.8	20,000	0.38	25.0	10.0

changes, evaporation and artificial water extraction as the main drainage of surface water in the area. The surface water along the tunnel line is mainly Jinji Lake water and Jinji Dun Park River water (connected with Jinji Lake), the lake surface elevation was measured several times during the survey, between September 24–27 due to continuous heavy rain, the water surface elevation up to 1.97 m, other non-rainy hours the water surface elevation is generally between 1.39–1.41 m. According to the field measurement, the water depth of K1+206–K1+250 in the west section of the tunnel main line is between 0.75 and 4.9 m, the water depth of K1+250–K3+860 in the middle section of the lake is between 3.7 and 5.71 m, and the water depth of K3+860–K4+080 in the east section of the lake is between 0.48 and 3.7 m.

- Diving is mainly located in the pore space of the shallow ①1 middle and lower sections of the miscellaneous fill and ①3 vegetal fill layer, with poor water-richness. Its recharge is mainly atmospheric precipitation and the surrounding lake (river) network system, with atmospheric evaporation and runoff to the surrounding lake (river) channel as its main discharge method. During the survey, the diving stable water level elevation was measured between 1.16 and 1.41 m. The rainfall in Suzhou area is mainly concentrated in June to September, during which the groundwater level is generally the highest; the dry season is from December to March, during which the groundwater level is generally the lowest. The annual water level variation is 1.00 m. According to the regional hydrological data, the highest dive level elevation in Suzhou is 2.63 m and the lowest dive level elevation is 0.21 m.
- The micro-pressure water is mainly stored in ③3 powder soil and ④2 powder soil sand layer, and the water distribution is average to good. Its recharge source is mainly the vertical infiltration of upper diving and lateral recharge of surrounding rivers, and the lateral runoff to the surrounding lake (river) network is its main discharge method. Due to the influence of topography and geomorphology, the initial water level and stable water level of the micro-pressure water level vary slightly. According to the results of two sets of pumping tests by the survey unit on both sides of Jinji Lake, the measured micro-head elevation in the west of the lake is 1.40 m, and the head elevation in the east of the lake is 1.45 m (due to soil extraction in the lake, the lake water directly replenishes the micro-head aquifer, resulting in the lake surface elevation being the same as or close to the micro-head elevation), it is suggested that the micro-head elevation in the west section of the lake and the water in the lake should be taken as 1.40 m, and the land area in the east of the lake should be taken as 1.45 m. The value is taken.
- The pressurized water in the pressurized water zone is mainly stored in ⑦2 powder sand layer, and there are ⑥2 powder clay and ⑥4 powder clay layers, which are connected with ⑦2 powder sand layer, and they are both pressurized water aquifers with medium to good water richness. The aquifer has relatively good confinement conditions, and the source of recharge is mainly

the overflow recharge of pressurized water and subsurface runoff recharge, with subsurface runoff and artificial pumping as the main drainage methods. According to the regional hydrogeological data, the change of water level of pressurized water is generally about 1 m. According to the data of pressurized water pumping test in the east and west of Jinji Lake, the head elevation of pressurized water in the west of the lake is –1.58 m, and the head elevation in the east of the lake is –1.42 m.

3. Numerical modeling

3.1. Cofferdam structure

The cofferdam of Suzhou Jinji Lake is a bilateral cofferdam, but because the south and north cofferdams are more than 300 m apart, the mutual influence is very small, and in order to streamline the calculation, one side of the cofferdam is selected to establish a numerical model for deformation analysis. Since the south side cofferdam structure is closer to the excavation of the foundation pit within the weir, it poses a great hidden danger to the safety of the cofferdam support process, so the south side cofferdam of Jinji Lake was selected for the study, and since the water depth outside the weir is the main factor affecting the safety of tunnel support, the cofferdam section at the deepest water level in the south side cofferdam lake (south side cofferdam S1+284 section) was selected for the simulation study. The cofferdam section and cofferdam structure plan layout are shown in Figs. 2 and 3.

The cofferdam structure of this project adopts the form of PC combined method pile + steel pipe pile, the combination pile of 720 mm outer diameter steel pipe pile (wall thickness 12 mm) + Larsen VI type steel sheet pile. Combined pile plan diagram and combined pile sample diagram are shown in Fig. 4.

3.2. Finite element model

MidasCivil finite element software was used to establish the deformation analysis model of the pumping process of PC combined engineering pile cofferdam support structure in deep water area. The geometric parameters of the source model are as follows: the geometric model of the lake bottom soil body with length, width and height of 60, 30 and 30 m, respectively is established. The length of the steel pipe pile on the pit side is 18 m, the embedded depth is 9.226 m, and the cantilever length is 8.774; the length of the locking steel pipe pile and the steel sheet pile on the waterward side are both 23 m, the embedded depth is 14.226 m, and the cantilever length is 8.774 m. The distance between the rows of double-row piles is 7 m; the length of the tie bars is 7 m, and the upper and lower ties are set at 0.5 m and 1.15 m below the top of the piles, respectively. The length, width and height of the geometric model of the weir core between the double rows of piles are 30, 7 and 9.274 m, respectively. It is assumed that the initial water depth of both the waterward side and the pit side of the PC combined method pile weir support structure are 7 m. The weir model is shown in Fig. 5, and the structure of the double rows of piles and ties is shown in Fig. 6.

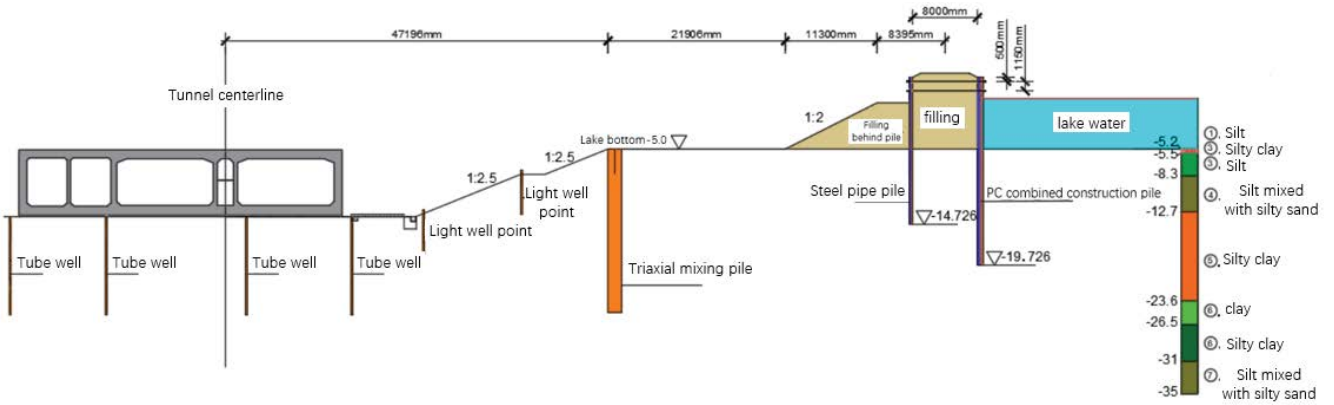


Fig. 2. Standard cross-section of cofferdam.

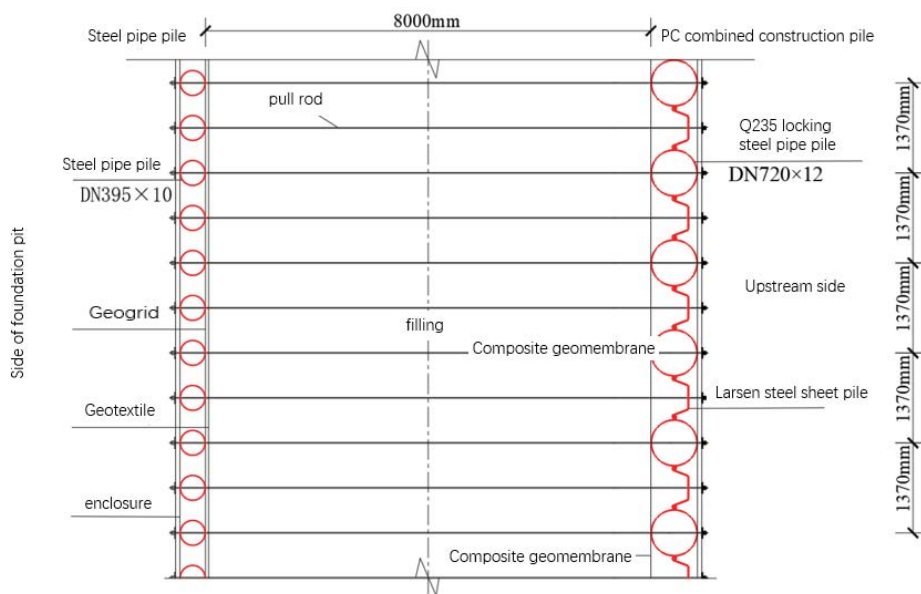


Fig. 3. Cofferdam structure plan layout.



Fig. 4. Schematic diagram of PC combined method pile cofferdam.

3.3. Analysis of working conditions

The construction process of pumping water inside the cofferdam at the project site was divided into seven working conditions for simulated construction, as shown in Table 2.

The weir pumping completion calculation model is shown in Fig. 7.

3.4. Analysis of calculation results

3.4.1. Horizontal displacement analysis of the cofferdam support system

Fig. 8 shows the horizontal displacement clouds of the cofferdam support structure under all construction conditions of the pumping obtained by the numerical simulation software.

As can be seen from Fig. 8: the pumping process on the inner side of the weir leads to horizontal displacement of the weir structure toward the backwater side of the weir, so in the actual construction, emphasis should be placed on monitoring the deformation of the weir structure during the construction process in both weirs and taking timely targeted measures. The horizontal displacement at the bottom of the fill behind the weir is the largest after

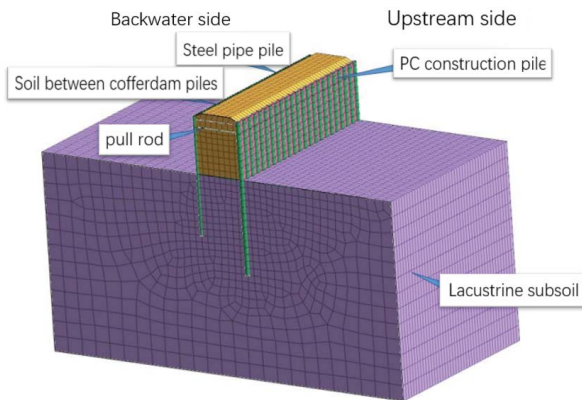


Fig. 5. Front view of the model.

the completion of the excavation of the slope release of the foundation pit inside the weir.

In order to analyze the deformation law of the cofferdam piles in detail, the deformation of the front and rear rows of steel pipe piles after the end of pumping in the weir deformation clouds of steel pipe piles are analyzed. The horizontal displacement of the front and rear rows of steel pipe piles under each working condition was extracted by MidasCivil software and plotted in Fig. 9; the horizontal displacement of the top of the front and rear rows of steel pipe piles under each working condition was extracted and plotted in Fig. 10.

It can be seen that when pumping is carried out inside the cofferdam, the water pressure inside the cofferdam will keep decreasing and the difference between the internal and external water pressure keeps increasing, which leads to the tendency of the cofferdam as a whole to move towards the inner side of the pit under the action of the water pressure outside the cofferdam. With the continuous pumping construction in the pit, the horizontal displacement of the top of the front and rear rows of piles gradually increases. After all the pumping was finished, the horizontal displacement of the top of the steel pipe pile on the backwater side and the PC combined method pile on the waterward side were -18.88 and -19.31 mm, respectively.

During the pumping construction in the cofferdam, the maximum point of horizontal displacement deformation of steel piles on both sides of the cofferdam is roughly

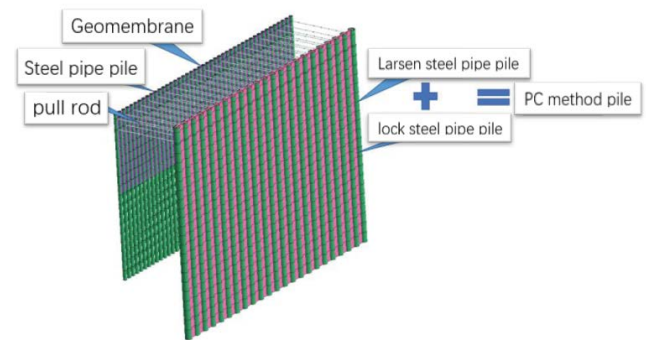


Fig. 6. Double-row pile and tie structure diagram.

Table 2
Simulated construction work conditions

Working condition	Description of model calculation process
Initial geostress state	Activate all soil elements, soil weight, water level distribution, displacement boundary, locking steel pipe pile, steel sheet pile, steel pipe pile activate all soil elements, soil weight, water level distribution, displacement boundary, locking steel pipe pile, steel sheet pile, steel pipe pile, and tie rod, and check the displacement reset option at the same time
Water pumping 1 m at the back side of cofferdam	Add corresponding water pressure
Water pumping 2 m at the back side of cofferdam	Add corresponding water pressure
Water pumping 3 m at the back side of cofferdam	Add corresponding water pressure
Water pumping 4 m at the back side of cofferdam	Add corresponding water pressure
Water pumping 5 m at the back side of cofferdam	Add corresponding water pressure
Water pumping 6.2 m at the back side of cofferdam	Add corresponding water pressure

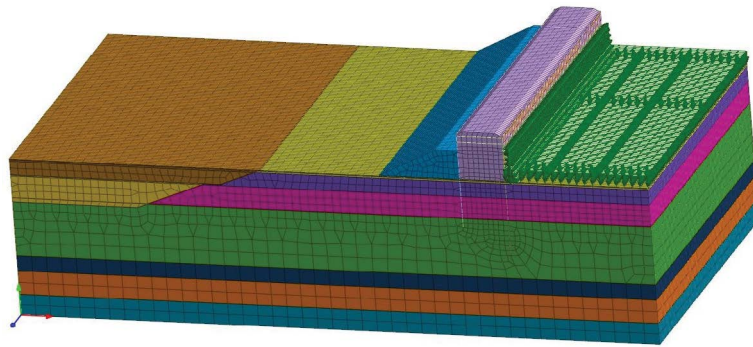


Fig. 7. Cofferdam backwater side pumping completion calculation model.

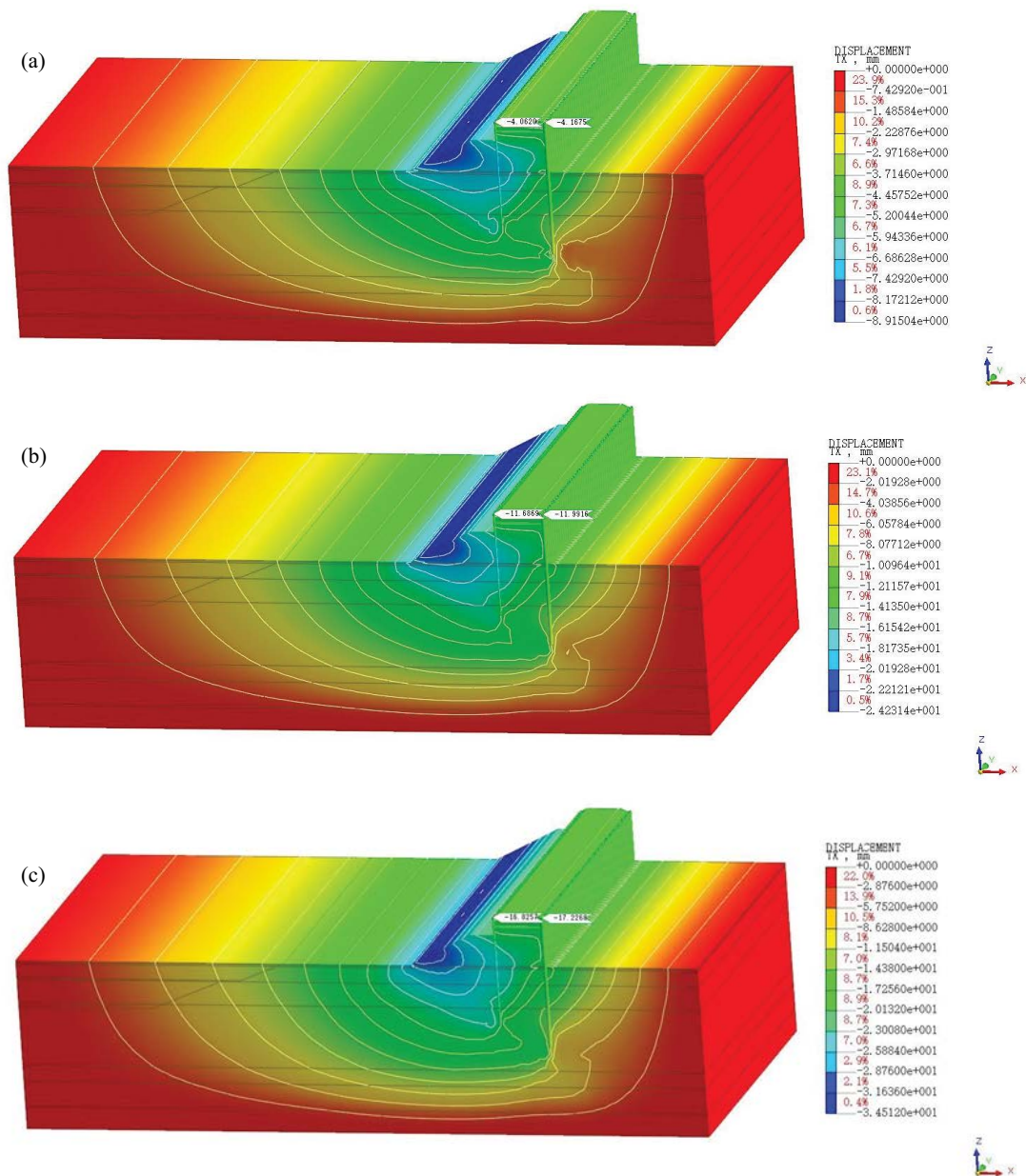


Fig. 8. Horizontal displacement clouds of the cofferdam support structure under (a) 1 m, (b) 3 m, and (c) 5 m working conditions of water pumping.

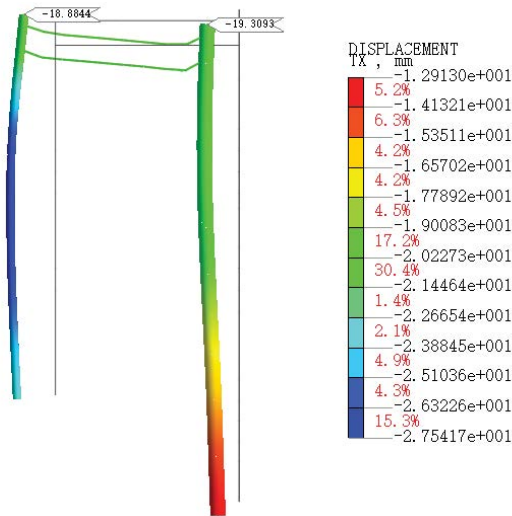


Fig. 9. Horizontal displacement of the double-row pile after the end of pumping.

at the position near the bottom surface of the lake, and the difference between the horizontal displacement value of the top of the PC method pile on the waterward side and the maximum value of the horizontal displacement of the pile is not large, but the difference between the horizontal displacement value of the top of the steel pipe pile on the backwater side and the maximum value of the horizontal displacement of the pile is large. The horizontal displacement ratio of the top of the double-row pile in the pumping stage is 6:4, and the pumping stage makes the most obvious deformation of the cofferdam support structure.

3.4.2. Horizontal displacement analysis of the cofferdam support system

Fig. 11 shows the vertical displacement clouds of the cofferdam support system under all construction conditions of the pumping obtained by the numerical simulation software.

As can be seen from Fig. 11, the pumping process of the cofferdam leads to the settlement of the lake bottom on the waterward side and the soil between the piles of the cofferdam, resulting in the uplift of the soil at the lake bottom on the backwater side. With the increase of the pumping depth, the settlement of the soil between the piles gradually increases. It can also be seen that at the end of pumping, the maximum settlement of the top of the inter-pile soil near the waterward side is 16.05 mm. The vertical displacement of the top of the double-row pile under each working condition is shown in Fig. 12.

As can be seen from Fig. 12, the vertical displacement of the top of the front and rear rows of piles gradually increases with the pumping of water on the backwater side of the cofferdam. After all the pumping is finished, the vertical displacement of the top of the piles of the steel pipe pile on the backwater side and the PC combined method pile on the waterward side are -2.66 and -8.68 mm, respectively.

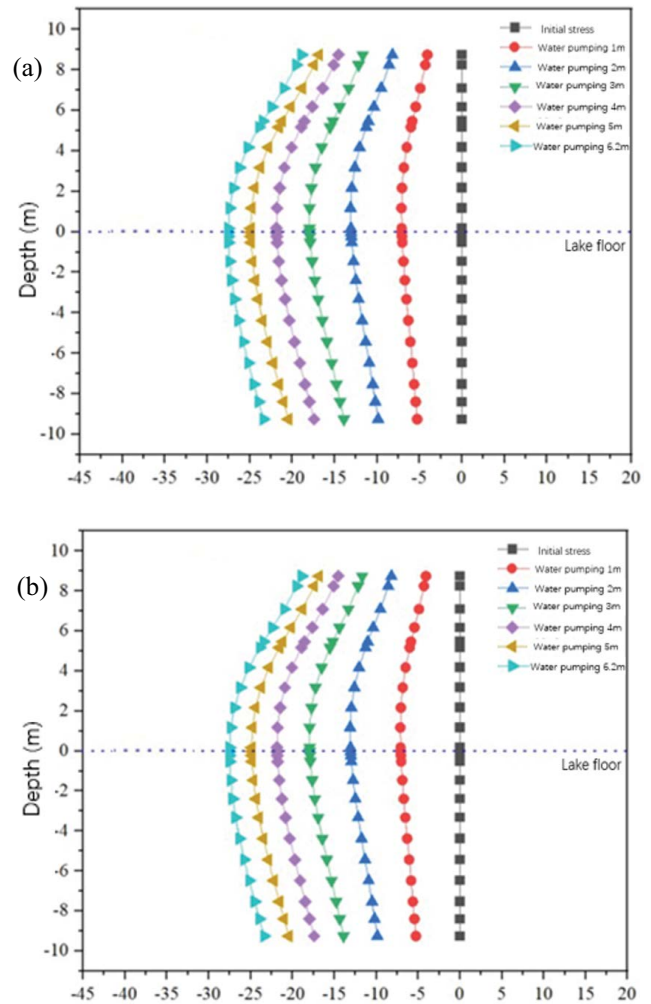


Fig. 10. Horizontal displacement diagram of (a) steel pipe pile shaft at backwater side (mm) and (b) PC combined construction pile shaft at the upstream side (mm).

3.4.3. Tie rod shaft force analysis

The axial force cloud of the tie rod at the end of the precipitation is shown in Fig. 13.

The maximum axial force of the ties at the upper level after the end of precipitation was 43 kN, and the maximum axial force of the ties at the lower level after the end of precipitation was 31.04 kN. The deformation of the ties was within the allowable range for safe construction.

4. Site monitoring and construction period deformation analysis

4.1. On-site monitoring

The project is located in Jinji Lake, with large cofferdam construction, and all the rest of the works are carried out in the cofferdam; the project monitoring work is based on national and local specifications, etc. For the monitoring of the cofferdam, the following enhancement measures are taken.

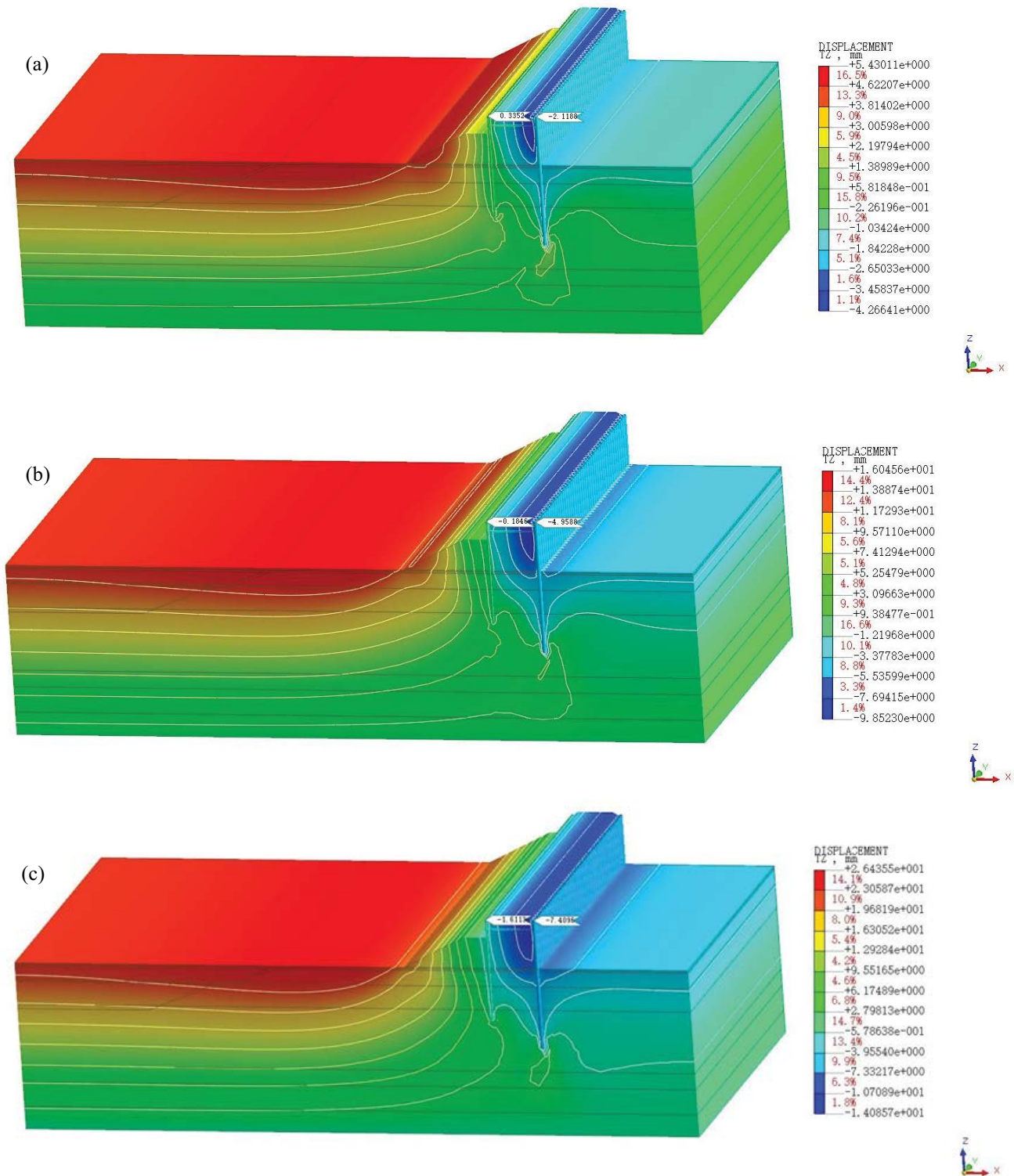


Fig. 11. Vertical displacement clouds of the cofferdam support structure under (a) 1 m, (b) 3 m, and (c) 5 m working conditions of pumping.

- The horizontal displacement of the top of the cofferdam pile and the axial force of the cofferdam ties in the cofferdam monitoring project are proposed to be monitored by automated methods in order to grasp the deformation of the cofferdam in a real-time and dynamic manner.
- For the horizontal displacement monitoring of the top of the cofferdam, in order to overcome the special

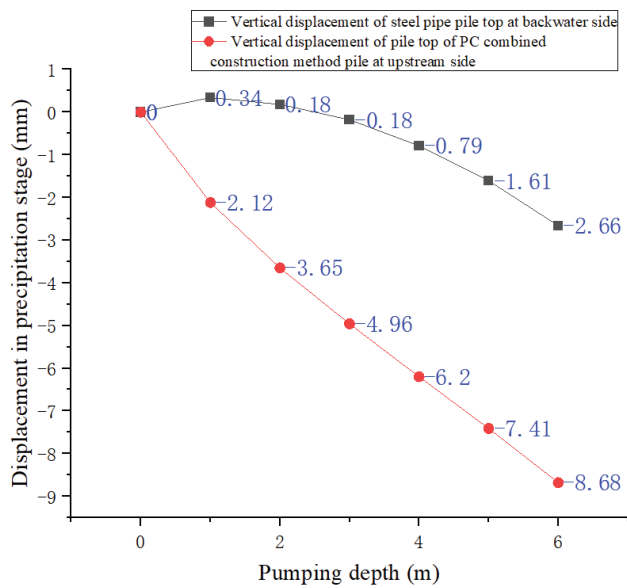


Fig. 12. Comparison of vertical displacement of double-row pile tops under various pumping conditions.

situation of large span and lack of reliable reference points in this project area as well as to obtain high measurement accuracy, it is proposed to adopt a two-level monitoring network combining absolute positioning and relative positioning.

- Strengthen the inspection of the cofferdam and slope release surface, especially for the presence of water leakage and cracks, and report and encrypt the monitoring in time once abnormalities are found.

Considering the monitoring requirements of relevant codes and design documents, the specific monitoring items of this project are shown in Table 3, and the layout of monitoring points is shown in Fig. 14.

4.2. Construction period deformation analysis

I-ZD is the settlement of the cofferdam pile, I-WD is the horizontal displacement of the cofferdam pile, I-ZL is the axial force of the tie rod, and ZL-S1+300 is the axial force of the cofferdam pile. The entire monitoring work will be carried out based on the construction conditions and changes in the monitored objects [30], and a combination of timing and tracking will be adopted. The monitoring

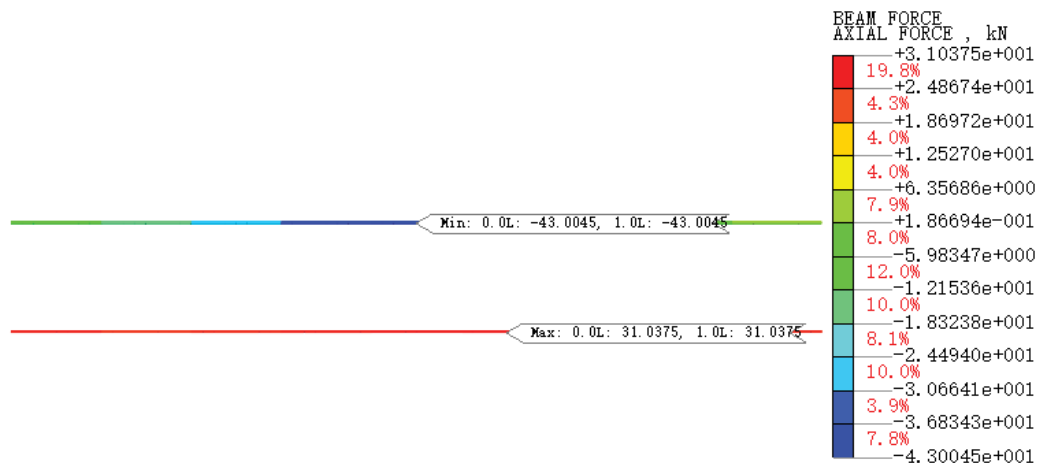


Fig. 13. Tie rod axial force cloud after the end of precipitation.

Table 3
Monitoring project layout

Monitoring items	Layout position	Monitoring tools	Requirements for measuring point layout
Horizontal displacement of pile top	Top of steel pipe pile	Total station	Monitoring control point of weir top displacement is arranged at the center of the cofferdam top with a longitudinal spacing of 150 m
Settlement of pile top	Top of steel pipe pile	Level	19.3
Pull rod axial force	Pull rod	Strain gauge	In the middle of pull rod, the distance between monitoring control points is 300 m. It is arranged on the tie rod
Water level outside weir	Steel sheet pile shaft	Water level gauge	Select one pile
Water level in weir	Steel sheet pile shaft	Water level gauge	Select one pile
Weir crest settlement	Center line of weir crest	Total station	Cofferdam center is arranged every 150 m

work of this project starts from the completion of the cofferdam construction, before pumping, and ends after the cofferdam is removed.

By integrating and analyzing the data of the 10 horizontal displacement monitoring points in Fig. 15, it is found that the horizontal displacement evolution pattern of the monitoring points are all consistent, and there is no situation of unreliable data due to the damage of the monitoring points, and all 10 horizontal displacement monitoring points are effective monitoring points.

Data analysis of Fig. 15 shows that the horizontal displacement of the pile top on the waterward side of the

PC combined method pile cofferdam increases with the increase of pumping depth and slope excavation depth inside the weir, and the horizontal displacement of the pile top on the waterward side reaches the maximum value after the completion of slope excavation construction. After the completion of the slope release excavation in the weir, the horizontal displacement of the pile top on the waterward side of the cofferdam shows a small deformation rebound and finally reaches its own stable state. In the weir pumping stage, the horizontal deformation value and horizontal deformation rate of the water-front side of the cofferdam are the largest, followed by the weir slope release excavation

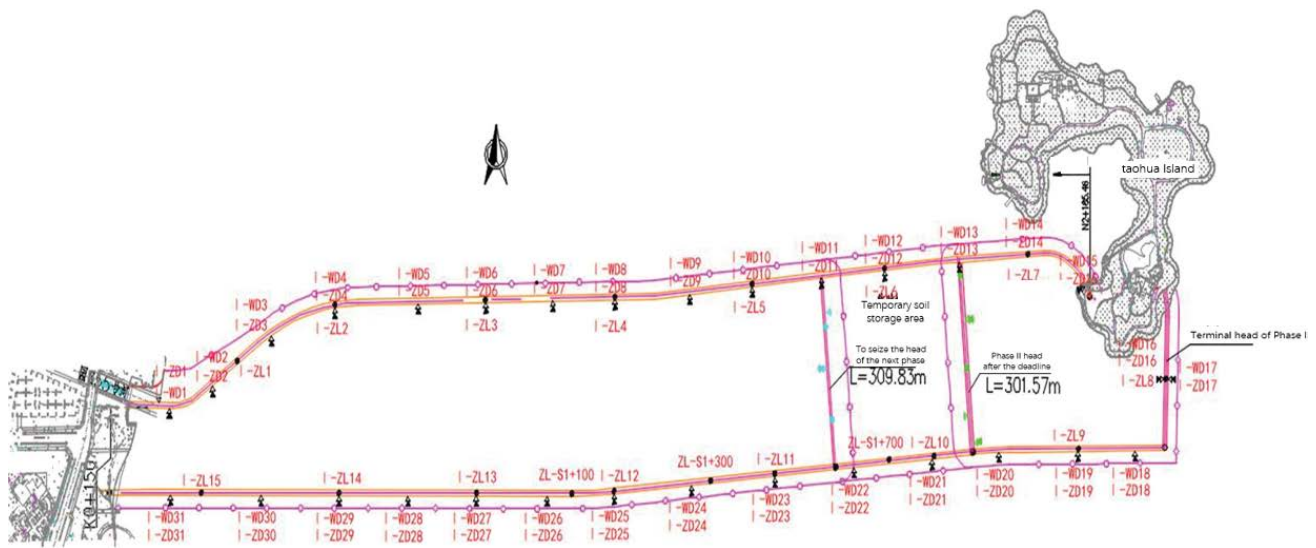


Fig. 14. Monitoring point layout.

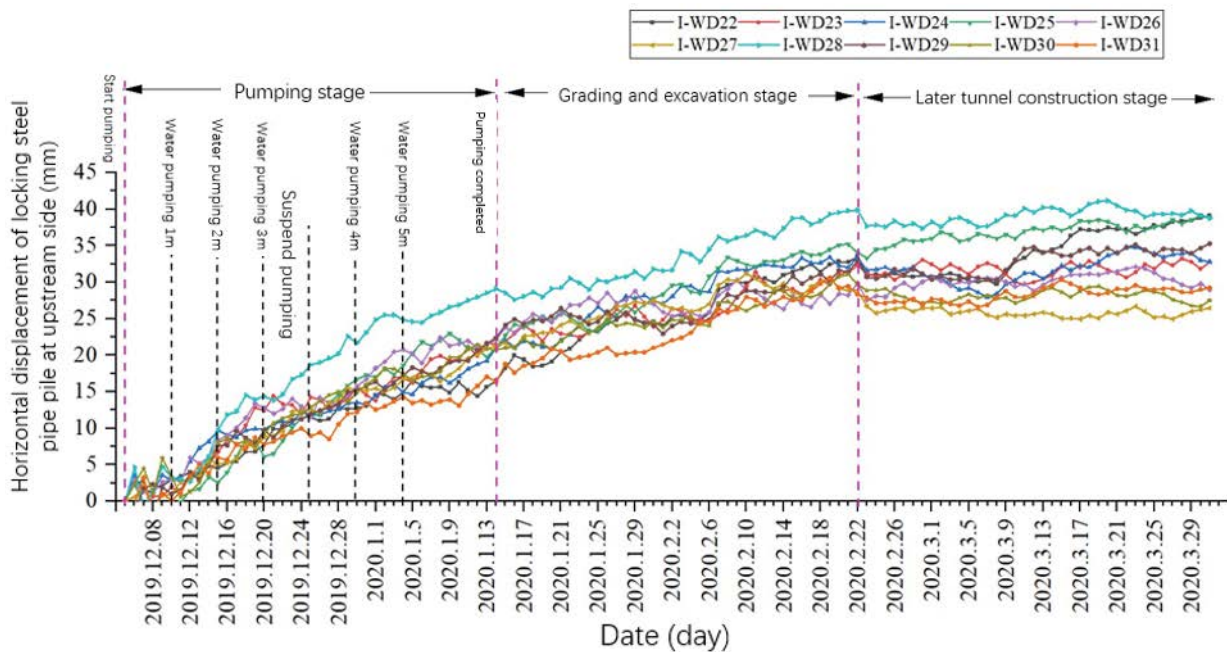


Fig. 15. Horizontal displacement of the top of PC combined work pile on the waterward side of monitoring points I-WD22-I-WD31.

stage, and the horizontal displacement of the cofferdam structure has basically stabilized after the completion of the weir slope release excavation construction.

Three horizontal displacement monitoring points on the waterward side of I-WD23–I-WD25 near section S1+284 of the south cofferdam were selected for detailed analysis. When the pumping construction in the weir is completed, the horizontal displacement monitoring values of the pile tops of I-WD23, I-WD24 and I-WD25 are 21.44, 20.93 and 21.05 mm, respectively; when the excavation construction in the weir is completed, the horizontal displacement monitoring values of the pile tops of I-WD23, I-WD24 and I-WD25 are 32.31, 33.43 and 34.07 mm.

In the whole process of pile top horizontal displacement deformation, the maximum deformation values of three monitoring points I-WD23, I-WD24 and I-WD25 are 33.07, 34.83 and 39.17 mm, respectively, and the maximum deformation rate is 4.87 mm/d, which are all much smaller than the pile top horizontal displacement of 130 mm and the maximum deformation rate is 4.87 mm/d, which is much less than the warning control standard of 130 mm and 5 mm/d.

In this paper, the horizontal displacement of the top of steel pipe pile on the backwater side is taken from I-WDJM22 to I-WDJM30 on the south side of the cofferdam of this project, and the data of a total of 9 points are plotted in Fig. 16.

By integrating and analyzing the data of the nine horizontal displacement monitoring points in Fig. 16, it is found that the horizontal displacement evolution pattern of the monitoring points is consistent, and there is no situation of unreliable data due to the damage of the monitoring points, and the nine horizontal displacement monitoring points are all effective monitoring points.

Data analysis of Fig. 16 shows that the horizontal displacement of the top of the steel pipe pile on the backwater

side of the cofferdam increases with the increase of pumping depth and slope excavation depth in the weir, and the horizontal displacement of the top of the pile on the backwater side reaches the maximum value after the completion of slope release excavation construction. After the completion of slope release excavation, the horizontal displacement of pile top on the backwater side of the cofferdam shows a small deformation rebound and finally reaches its own stable state. In the weir pumping stage, the horizontal deformation value and horizontal deformation rate of the backwater side of the cofferdam are the largest, followed by the weir slope release excavation stage, and the horizontal displacement of the cofferdam structure has basically stabilized after the completion of the weir slope release excavation construction.

Three backwater-side horizontal displacement monitoring points, I-WDJM23–I-WDJM25, near section S1+284 of the south cofferdam, were selected for detailed analysis. At the completion of the pumping construction in the weir, the horizontal displacement monitoring values of the pile tops of I-WDJM23, I-WDJM24 and I-WDJM25 were 18.14, 17.39 and 20.16 mm, respectively; at the completion of the slope release excavation construction in the weir, the horizontal displacement of the pile tops of I-WDJM23, I-WDJM24 and I-WDJM25 were 34.78, 31.25 and 37.42 mm, respectively, and the maximum deformation rate is 3.75 mm/d, all of which are much smaller than the maximum deformation values of 130 and 37.42 mm. The maximum deformation rate is 3.75 mm/d, which is much less than the warning control standard of 130 mm and 5 mm/d of horizontal displacement of pile top.

By integrating and analyzing the data of the 10 vertical displacement monitoring points in Fig. 17, it was found that the evolution pattern of vertical displacement of the monitoring points all remained consistent, and there was no case of unreliable data due to the damage of the

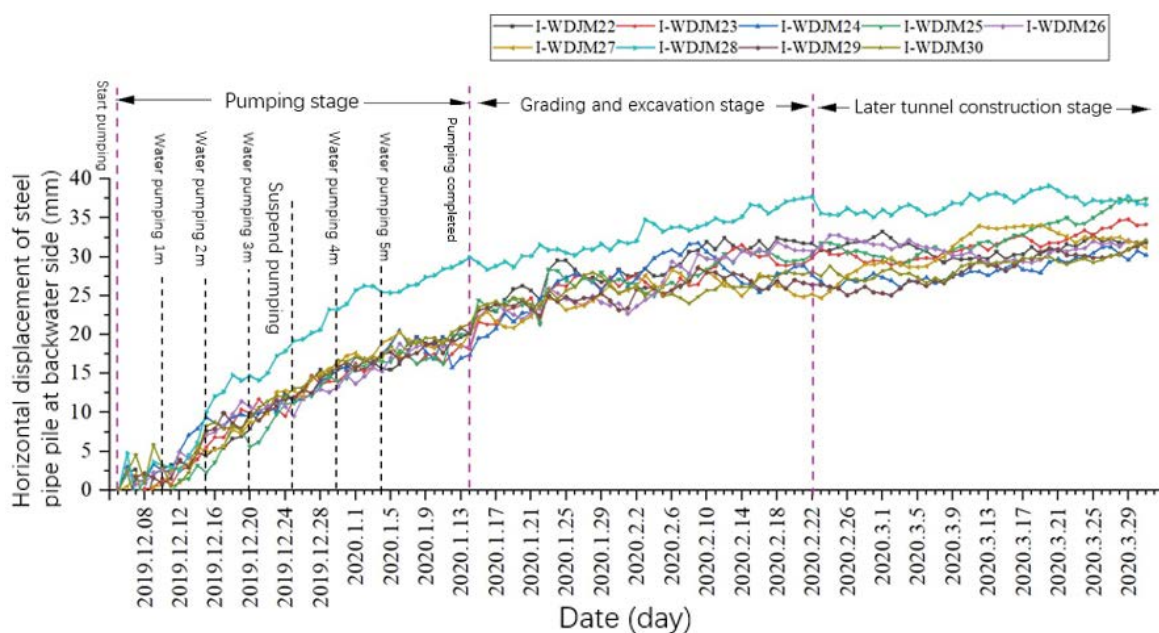


Fig. 16. Horizontal displacement of steel pipe pile tops on the backwater side of monitoring points I-WDJM22–I-WDJM30.

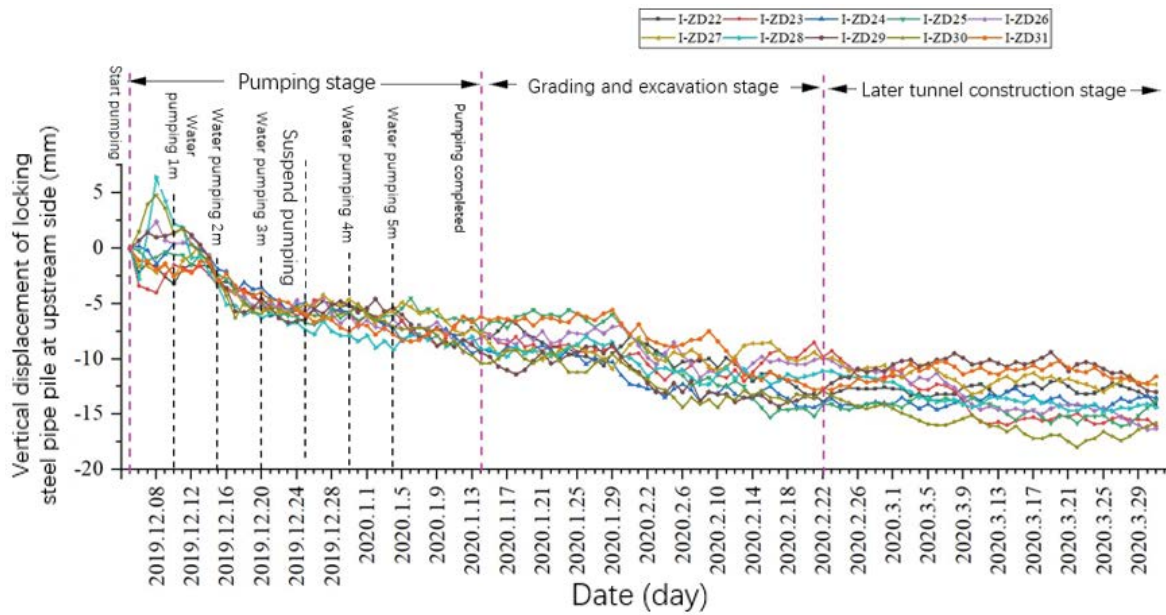


Fig. 17. Vertical displacement of the top of PC combined work pile on the waterward side of monitoring points I-ZD22–I-ZD31.

monitoring points, and all 10 vertical displacement monitoring points were valid monitoring points.

Data analysis of Fig. 17 shows that the vertical displacement of the pile top on the waterward side of the PC combined method pile cofferdam increases with the increase of pumping depth and slope excavation depth inside the weir, and the vertical displacement of the pile top on the waterward side reaches the maximum value after the completion of slope excavation construction. After the completion of the slope release excavation, the vertical displacement of the pile top on the waterward side of the cofferdam shows a small deformation rebound and finally reaches its own stable state. In the pumping stage of the weir, the percentage of vertical displacement value and the rate of vertical displacement change on the waterward side of the weir are the largest, followed by the excavation stage of the weir slope release, and the vertical displacement of the weir structure has basically stabilized after the completion of the weir slope release excavation construction.

Three waterward side vertical displacement monitoring points, I-ZD23–I-ZD25, near section S1+284 of the south cofferdam, were selected for detailed analysis. At the completion of pumping construction in the weir, the monitoring values of vertical displacement of pile tops at three monitoring points of I-ZD23, I-ZD24 and I-ZD25 were -7.5 , -9.1 and -7.5 mm, respectively; at the completion of slope release excavation construction in the weir, the monitoring values of vertical displacement of pile tops at three monitoring points of I-ZD23, I-ZD24 and I-ZD25 were -9.8 , -14 and -14.1 mm, respectively. During the whole process of pile top vertical displacement deformation, the maximum vertical displacement monitoring values of I-ZD23, I-ZD24 and I-ZD25 are -16.1 , -14.7 and -15.8 mm, respectively, with the maximum change rate of 3.4 mm/d, which are much smaller than the warning standard of pile top vertical displacement of 130 mm and 5 mm/d control standard.

By integrating and analyzing the data of the nine vertical displacement monitoring points in Fig. 18, it was found that the evolution pattern of vertical displacement of the monitoring points all remained consistent, and there was no case of unreliable data due to the damage of the monitoring points, and all nine vertical displacement monitoring points were valid monitoring points.

Data analysis of Fig. 18 shows that the vertical displacement of the pile top of the steel pipe pile on the backwater side of the cofferdam increases with the increase of pumping depth and slope excavation depth in the weir, and the vertical displacement of the pile top on the backwater side reaches its maximum value after the completion of slope excavation construction. After the completion of the slope release excavation, the vertical displacement of the pile top on the backwater side of the cofferdam shows a small deformation rebound and finally reaches its own stable state. In the pumping stage of the weir, the percentage of vertical displacement value and vertical displacement change rate of the backwater side of the cofferdam are the largest, followed by the slope release excavation stage in the weir, and the vertical displacement of the cofferdam structure has basically stabilized after the completion of the slope release excavation construction in the weir.

Three backwater-side vertical displacement monitoring points, I-ZDJM23–I-ZDJM25, near the southern cofferdam S1+284 section, were selected for detailed analysis. At the completion of the pumping construction in the weir, the monitoring values of the vertical displacement of the pile tops of I-ZDJM23, I-ZDJM24 and I-ZDJM25 were -3.87 , -4.95 and -5.04 mm, respectively; at the completion of the slope release excavation construction in the weir, the monitoring values of the vertical displacement of the pile tops of I-ZDJM23, I-ZDJM24 and I-ZDJM25 were -9.8 , -14 and -14.1 mm, respectively. During the whole process of vertical displacement deformation, the maximum vertical displacement monitoring values of I-ZDJM23,

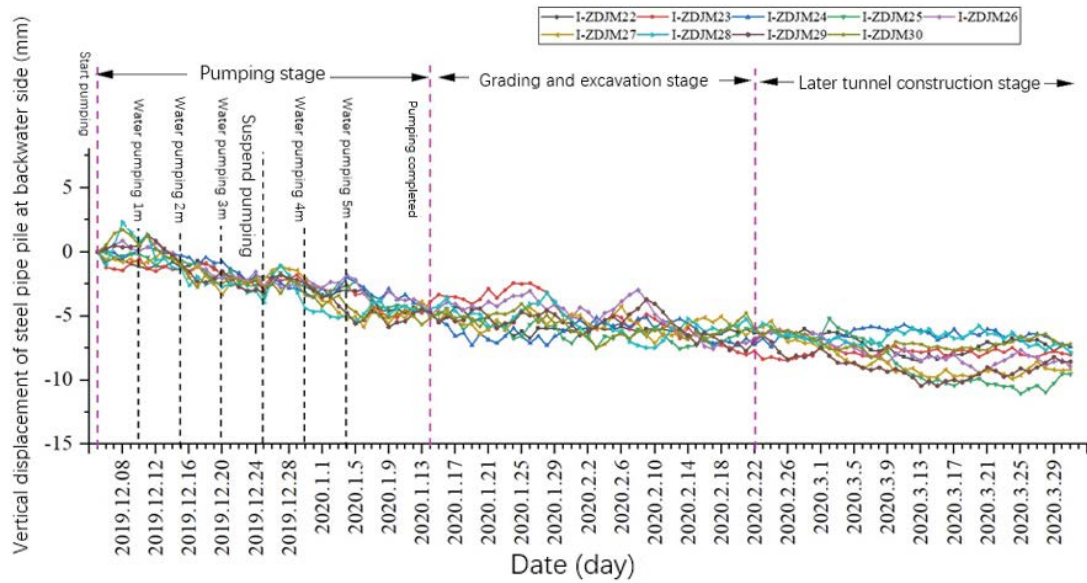


Fig. 18. Vertical displacement of steel pipe pile tops on the backwater side of monitoring points I-ZDJM22-I-ZDJM30.

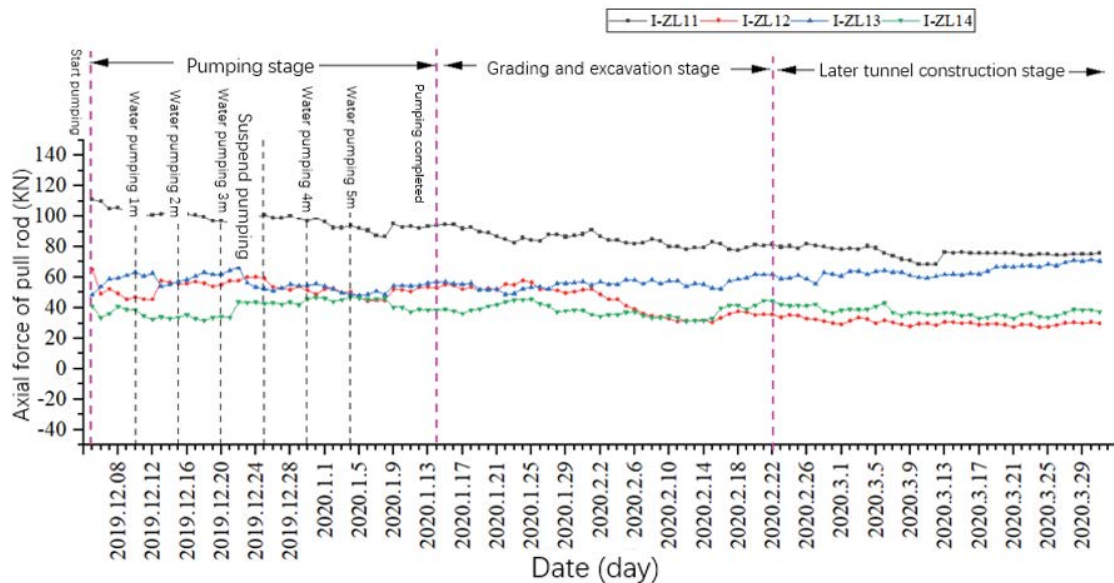


Fig. 19. Tie rod axial force at monitoring points I-ZL11-I-ZL14.

I-ZDJM24 and I-ZDJM25 are -8.46 , -7.38 and -11.04 mm, respectively, and the maximum change rate is -1.22 mm/d. The maximum change rate is -1.22 mm/d, which is much smaller than the warning control standard of 130 mm and 5 mm/d of vertical displacement of pile top.

By integrating and analyzing the data of the four monitoring points of tie rod axial force in Fig. 19, it was found that the evolution pattern of the tie rod axial force of the monitoring points remained consistent, and there was no unreliable data due to the damage of the monitoring points, and the four monitoring points of tie rod axial force are all effective monitoring points.

Data analysis of Fig. 19 shows that the tie rod axial force is larger at the beginning of the pumping stage, and

then maintains stable fluctuations with the increase of pumping depth and slope release excavation depth in the weir. After the completion of the weir slope excavation, the axial force of the tie rod decreases and finally reaches its own stable state.

Four horizontal displacement monitoring points on the waterward side of I-ZL11-I-ZL14 near the S1+284 section of the south cofferdam were selected for detailed analysis. At the completion of pumping construction in the weir, the monitoring values of the tie rod axial force at four monitoring points of I-ZL11, I-ZL12, I-ZL13 and I-ZL14 are 94.16, 53.10, 57.14 and 38.48 kN, respectively; at the completion of slope release excavation construction in the weir, the monitoring values of the tie rod axial force at four

points of I-ZL11, I-ZL12, I-ZL13 and I-ZL14 are the maximum axial force values at four monitoring points, I-ZL11, I-ZL12, I-ZL13 and I-ZL14, were 81.64, 35.78, 61.88 and 44.36 kN, respectively during the change of the axial force of the ties, all of which are much smaller than the warning control mark of 315 kN for the cumulative variable of tie rod axial force.

5. Conclusions

In this paper, based on MidasCivil finite element software, the cofferdam deformation law and characteristics of the construction process of the inner pumping of the cofferdam at the project site were selected for simulation and analysis, and the project site monitoring values were compared with the numerical results, and the following conclusions were drawn.

- The comparison between the field monitoring data and the numerical simulation results is demonstrated. The final results and change trends of the field monitoring data and the numerical simulation data are basically consistent, which further verifies the accuracy of the numerical simulation results. The horizontal displacement and vertical displacement of the double-row pile increase continuously with the increase of the pumping depth in the weir, and the weir deformation gradually stabilizes after the completion of the pumping construction in the weir. The maximum horizontal displacement of the pile top and the maximum vertical displacement of the pile top are 39.17 and 16.1 mm, respectively, and the maximum axial force of the ties during the construction of the weir is 110.96 kN, which are much smaller than the warning control standard.
- When water is pumped inside the cofferdam, the water pressure inside the cofferdam decreases continuously, while the water pressure outside the cofferdam remains unchanged, resulting in the difference between the internal and external water pressure, which causes the overall structural deformation of the cofferdam to show a tendency to move toward the inside of the cofferdam. When the pit inside the cofferdam is released for excavation, the tendency of the overall structural deformation of the cofferdam to move toward the inside of the cofferdam is further intensified due to the joint action of the soil disturbance and the water pressure outside the cofferdam.
- With the continuous pumping in the weir, the horizontal displacement of the top of the front and rear rows of piles in the cofferdam gradually increases, and the vertical displacement of the top of the front and rear rows of piles also gradually increases.
- During the pumping process in the weir, the horizontal displacement values of the pile tops on the waterward and backward sides of the cofferdam do not differ much, and the maximum value of the horizontal displacement of the pile on the waterward side and the horizontal displacement value of its top also differ little, but the maximum value of the horizontal displacement of the pile on the backward side differs significantly from the horizontal displacement value of its top.

- For the horizontal displacement of the piles on both sides of the weir, the maximum point of displacement basically occurs near the bottom surface of the lake during the pumping process in the weir.

Statements and declarations

Conflicts of interest: None.

Funding: No funding was received for conducting this study.

References

- [1] A.F. Uribe-Henao, L.G. Arboleda-Monsalve, Sheet Pile Interlocks and Ring Beam Installation Effects on the Performance of Urban Cofferdams, *Geotechnical Frontiers*, American Society of Civil Engineers, Reston, VA, USA, 2017, pp. 170–180.
- [2] T.N. Quang, B.T. Anh, T.V. Cong, T.M. Cao, Combination of Cement Deep Mixing (CDM) and Steel Sheet Piles for the Cofferdam Used in Construction of Deep Foundation Pit in Soft Ground in the Mekong Delta Coast, *CIGOS 2021, Emerging Technologies and Applications for Green Infrastructure*, Proceedings of the 6th International Conference on Geotechnics, Civil Engineering and Structures, Springer Nature, Singapore, October 2021.
- [3] V.V. Verstov, A.F. Yudina, A.N. Gaido, Improving efficiency of arranging offshore cofferdams, *Soil Mech. Found. Eng.*, 57 (2020) 73–76.
- [4] P. Li, X. Sun, J. Chen, J. Shi, Effects of new construction technology on performance of ultralong steel sheet pile cofferdams under tidal action, *Geomech. Eng.*, 27 (2021) 561–571.
- [5] J. Wang, Z. Jiang, F. Li, W. Chen, The prediction of water level based on support vector machine under construction condition of steel sheet pile cofferdam, *Concurrency Comput. Pract. Exper.*, 33 (2021) e6003, doi: 10.1002/cpe.6003.
- [6] M.-W. Gui, K.-K. Han, An investigation on a failed double-wall cofferdam during construction, *Eng. Fail. Anal.*, 16 (2009) 421–432.
- [7] Y.-m. Hou, J.-h. Wang, Q.-y. Gu, Deformation performance of double steel sheet piles cofferdam, *J. Shanghai Jiaotong Univ.*, 43 (2009) 1577–1580, 1584.
- [8] C.-x. Huang, Y. Liu, Z.-w. Yao, J.-j. Li, Y. Xia, Research and application of double-row steel sheet pile stability in soft soil foundation, *J. Phys. Conf. Ser.*, 2029 (2021) 012082, doi: 10.1088/1742-6596/2029/1/012082.
- [9] B.L. Xiong, J.S. Tang, W. Chen, Inside and outside earth pressure research of steel sheet pile cofferdam, *Adv. Mater. Res.*, 446–449 (2012) 1822–1826.
- [10] J. Wang, H. Xiang, J. Yan, Numerical simulation of steel sheet pile support structures in foundation pit excavation, *Int. J. Geomech.*, 19 (2019) 05019002, doi: 10.1061/(ASCE)GM.1943-5622.0001373.
- [11] A. Liu, B. Li, J. Chen, C. Gao, Research and application of large diameter steel cylinder island construction technology in Hong Kong-Zhuhai-Macao Bridge Project, *Ships Offshore Struct.*, 16 (2021) 33–41.
- [12] J. Wu, Z. Zhou, W. Xia, H. Wang, Z. Fang, A novel excavation and construction method for an extra-long underwater tunnel in soft soils, *Adv. Civ. Eng.*, 2021 (2021) 6184411, doi: 10.1155/2021/6184411.
- [13] L.G. Arboleda-Monsalve, A.F. Uribe-Henao, A. Velásquez-Pérez, D.G. Zapata-Medina, F. Sarabia, Performance of urban cofferdams braced with segmental steel and reinforced concrete ring beams, *J. Geotech. Geoenviron. Eng.*, 144 (2018) 04018015, doi: 10.1061/(ASCE)GT.1943-5606.0001864.
- [14] A. Felipe Uribe-Henao, L.G. Arboleda-Monsalve, D. Alejandro Aguirre-Molina, D.G. Zapata-Medina, Construction-induced effects in a cofferdam excavation using Hypoplasticity and Shotcrete models, *Tunnelling Underground Space Technol.*, 124 (2022) 104446, doi: 10.1016/j.tust.2022.104446.

- [15] J. Spaans, G.V. Milutinovic, New lock at Kentucky dam: analysis and design of precast concrete cofferdams, *PCI J.*, 66 (2021) 23–40.
- [16] A. Pal, D. Potočnik, M. Vulić, Rock-fill cofferdam crest settlement behavior analysis through geodetic monitoring data, *Minerals*, 10 (2020) 152, doi: 10.3390/min10020152.
- [17] J.-B. Su, Z.-Y. Yu, Y.-R. Lv, Y.-H. Zhu, H.-Q. Wang, Differential settlement of intersecting buildings in an offshore reclamation project, *Adv. Civ. Eng.*, 2019 (2019) 9453620, doi: 10.1155/2019/9453620.
- [18] M. Fall, Z. Gao, B.C. Ndiaye, Three-dimensional response of double anchored sheet pile walls subjected to excavation and construction sequence, *Heliyon*, 5 (2019) e01348, doi: 10.1016/j.heliyon.2019.e01348.
- [19] W.R. Azzam, A.Z. Elwakil, Performance of axially loaded-piled retaining wall: experimental and numerical analysis, *Int. J. Geomech.*, 17 (2017) 04016049, doi: 10.1061/(ASCE)GM.1943-5622.0000710.
- [20] G. Zheng, Y. Wang, P. Zhang, X. Chen, W. Cheng, Y. Zhao, X. Li, Performances and working mechanisms of inclined retaining structures for deep excavations, *Adv. Civ. Eng.*, 2020 (2020) 1740418, doi: 10.1155/2020/1740418.
- [21] I.D. Lefas, V.N. Georgiannou, Analysis of a cofferdam support and design implications, *Comput. Struct.*, 79 (2001) 2461–2469.
- [22] J. Shao, Z. Fan, Y. Huang, Y. Zhan, Q. Cai, Multi-objective optimization of double-walled steel cofferdams based on response surface methodology and particle swarm optimization algorithm, *Structures*, 49 (2023) 256–266.
- [23] Q. Yi, B. Li, J. Duan, Simulation analysis of composite steel cofferdam based on ANSYS finite element method, *J. Simul.*, 9 (2021) 99–103.
- [24] S. Chen, Y. Wang, Y. Li, X. Li, P. Guo, W. Hou, Y. Liu, Deformation and force analysis of wood-piled island cofferdam based on equivalent bending stiffness principle, *Buildings*, 12 (2022) 1104, doi: 10.3390/buildings12081104.
- [25] Z. Xu, W. Xu, Safety Analysis of the Single-Walled Steel Suspension Box Cofferdam During Construction, 2010 IEEE International Conference on Industrial Engineering and Engineering Management, IEEE, Macao, China, 2010.
- [26] H.J. Kim, J.O. Choi, Suction penetration review of circular steel pipes by field test, *J. Korean Geotech. Soc.*, 36 (2020) 35–43.
- [27] X. Lu, Y. Luo, H. Ming, M. Zhou, X. Zhang, D. Liu, Stability of nonuniform large geotextile-reinforced cofferdam under seepage and excavation effects, *Int. J. Geomech.*, 23 (2023) 04022283, doi: 10.1061/IJGNALGMENG-7707.
- [28] S. Chen, Y. Li, P. Guo, X. Zuo, Y. Liu, H. Yuan, Y. Wang, Ultimate bearing capacity of bottom sealing concrete in underwater deep foundation PIT: theoretical calculation and numerical analysis, *Machines*, 10 (2022) 830, doi: 10.3390/machines10100830.
- [29] T.A. Madanayaka, N. Sivakugan, Simple solutions for square and rectangular cofferdam seepage problems, *Can. Geotech. J.*, 56 (2019) 730–745.
- [30] J. Wang, G. Liu, Study of the monitoring system for double row steel sheet pile cofferdam engineering, *Int. J. Wireless Mobile Comput.*, 23 (2022) 256–260.